# Accurate Full-Band Equivalent Circuits of Inductive Posts in Rectangular Waveguide

Tullio Rozzi, *Fellow, IEEE,* Franco Moglie, *Member, IEEE,* Antonio Morini, William Gulloch, and Marco Politi

*Abstract*—**Inductive posts of finite dimensions are currently employed for the precise realization of millimeter wave filters in waveguide. Although this structure constitutes a classical problem, no true wideband equivalent circuit seems to be available, that is, with elements dependent only on post geometry and, at the same time, capable of describing higher order mode interaction. The availability of such an equivalent circuit is a prerequisite for efficient CAD. We develop a rigorous wideband model, inclusive of near neighbor interaction, suitable for accurate filter synthesis and CAD by means of a desk-top computer. Three actual applications to the design of multipost filters are presented with practical results in excellent agreement with computer predictions. Computation times are such that the analysis can be effected in real time.**

## Introduction

THE EFFICIENT CAD synthesis of millimeter wave filters and matching networks is greatly enhanced by the adoption of accurate wideband equivalent circuits. These can be included, for instance, as building blocks in commercially available microwave design packages. A typical example is provided by the design of filters using inductive posts in waveguide. Although this structure has been widely investigated and employed [1]–[7], up to date accurate analysis, inclusive of near neighbor interaction, requires a fairly intensive computer effort that must be repeated hundred of times in the CAD process.

A true accurate, wideband equivalent network ought to account for all physical effects, such as higher order modes interaction, and contain only frequency independent elements. The latter must be directly expressible in terms of the geometrical parameters, i.e., normalized post width and thickness, by means of graphs or interpolatory functions that can be fed into a network analysis package.

The availability of such a model, not only eliminates the need of repeating the field analysis at each frequency point, but also lays the foundation for rigorous synthesis from a given prototype, as opposed to straightforward CAD. To this aim, we have developed a rigorous Ritz–Galerkin variational analysis of the post including *a priori* the correct edge condition. This reduces to three the maximum size of matrices to be considered. Moreover, we have explicitly extracted from the field analysis the frequency dependence of the post reactance. Consequently, we recover its full Foster representation with elements dependent only on geometry. For the convenience of the user, element values of the equivalent circuit are plotted versus post width for a number of thicknesses. Near neighbor interaction, where present, is taken care of by considering a four port representation of the post where the first higher order waveguide mode is taken as "accessible" [8]. All higher order modes are "lumped" in the post reactance.

As a result of this analytical approach, we achieve a dramatic reduction of the computer times involved. Finally, computed and measured data are compared for three different multipost filters at $K_A$ band.

## Analysis

The geometry of the discontinuity is shown in Fig. 1.

In view of the longitudinal symmetry, we consider even/odd excitation corresponding to placing a magnetic/electric wall at $z = s/2$.

Moreover, in view of the symmetry of the exciting $TE_{10}$ mode and of the discontinuity, a magnetic wall is located at $x = a/2$ and the problem is reduced to that of the $H$-plane step. The problem is described in terms of the $E_y$ component of the $TE_{n0}$ modes in the guide $z < 0$, normalized over a guidewidth $a/2$:

$$e_n = \frac{2}{\sqrt{a}} \sin \frac{n\pi}{a} x \qquad n = 1, 3, 5 \cdots \tag{1}$$

with characteristic impedances

$$Y_{on} = \frac{1}{\omega\mu_0} \sqrt{k_o^2 - \left(\frac{n\pi}{a}\right)^2} \tag{2}$$

and of the analogous modes in the guide $z > 0$, normalized over a guidewidth $d$

$$e_n' = \sqrt{\frac{2}{d}} \sin \frac{n\pi}{d} x \qquad n = 1, 2, 3, 4 \cdots \tag{3}$$

Manuscript received April 25, 1991; revised November 11, 1991.

T. Rozzi, F. Moglie, and A. Morini are with the Dipartimento di Elettronica ed Automatica, Universita di Ancona, Via Brecce Bianche, 60131, Ancona, Italy.

W. Gulloch and M. Politi are with Telettra S.p.A. Vimercate, Milan, Italy, Telettra S.p.A., Via Trento 30, Vimercate, Milano, Italy.

IEEE Log Number 9106772.

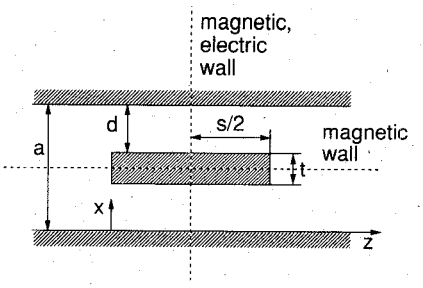


Fig. 1. Longitudinal view of the inductive post in rectangular waveguide.

with characteristic impedances

$$Y'_{on} = \frac{1}{\omega\mu_0}\sqrt{k_o^2 - \left(\frac{n\pi}{d}\right)^2} \tag{4}$$

It is expedient to normalize the working frequency as follows:

$$\bar{\omega} = \frac{\beta a}{\pi} = \sqrt{\left(\frac{ak_o}{\pi}\right)^2 - 1} \tag{5}$$

so that $\bar{\omega} = 0$ at the cutoff of the fundamental mode and $\bar{\omega} = \sqrt{3}$ at the cutoff of the first higher order mode in the larger guide ($TE_{20}$).

At the same time, we normalize all the characteristic impedances to that of the fundamental mode in the larger guide, so that we define in the larger guide:

$$y_{on} = Y_{on}/Y_{o1} = \frac{\sqrt{n^2 - 1 - \bar{\omega}^2}}{j\bar{\omega}} \tag{6}$$

and in the smaller guide:

$$y'_{on} = Y_{on}/Y_{o1} = \frac{\sqrt{n'^2 - 1 - \bar{\omega}^2}}{j\bar{\omega}} \quad \text{where} \quad n' = \frac{na}{d} \tag{7}$$

and the driving point admittances of the stub of length $s/2$ under magnetic/electric wall conditions at $z = s/2$ are given by

$$y'_n = y'_{on}\begin{cases}\tanh \gamma'_n s/2 \\ \coth \gamma'_n s/2\end{cases} \tag{8}$$

respectively, where

$$\gamma'_n = \frac{\pi}{a}\sqrt{n'^2 - 1 - \bar{\omega}^2}.$$

We are now in a position to form the admittance function of the step problem at $z$ at 0 as the sum of those of the semi-infinite guide to the left and of the guide stub to the right for the even/odd excitation cases. This takes the standard form:

$$\tilde{Y}(x, x') = \sum_{\substack{n > n_a \\ \text{odd}}}^{\infty} y_{on} e_n(x)\, e_n t(x') + \sum_{n=1}^{\infty} y'_n e'_n(x)\, e'_n(x') \tag{9}$$

with $y_n$, $y'_n$ defined in (6), (8) $e_n$, $e'_n$ in (1), (3) respectively.

The first summation excludes the 'accessible modes' ($n = 1, \cdots, n_a$) in the guide left of the step. We can now proceed to set up the integral equation of the step in a standard manner. By using the continuity of $E_y$ at both sides of the step we eliminate the modal amplitudes of all but the accessible modes in terms of the unknown $E_y$. Continuity of $H_x$ yields

$$\sum_{m=1}^{n_a} I_m e_m(x) = \int_0^d dx'\, \tilde{Y}(x, x')\, E_y(x'). \tag{10}$$

Where $I_1, \cdots, I_{na}$ are the amplitudes of $H_x$ for the accessible modes, that is $n_a = 1$ at least and, possibly, $n_a = 3$, in cases where the guide is oversize or near neighbor interaction between successive ports occurs.

By setting $I_m = 1$ and the remaining amplitudes equal to zero, we obtain $(n_a + 1)/2$ integral equations defining the discontinuity field $E_m(x)$ set up by the excitation of each accessible mode in turn, $m = 1, \cdots, n_a$:

$$e_m(x) = \int_0^d dx'\, \tilde{Y}(x, x')\, E_m(x') \tag{11}$$

In order to solve (11) efficiently, it is also expedient to turn it into a singular integral equation. Recalling that $E_y$ vanishes like $r^{2/3}$ at the discontinuous edge $x = d$, the above purpose is achieved by integrating (11) by parts with respect to $x$, so that the new unknown $dE_m/dx$ assumes a $r^{-1/3}$ singular behavior at $x = d$ instead. That is, from (11), by indefinite integration with respect to $x$ and integration by parts with respect to $x'$, one obtains:

$$\int dx\, e_m(x) = \int dx \int_0^d dx' \left(\int d\xi\, \tilde{Y}(x, \xi)\, \frac{dE_m(x')}{dx'}\right) \tag{12}$$

or, explicitly,

$$\frac{1}{m}\phi_m(x) = \sum_{\substack{n > n_a \\ \text{odd}}}^{\infty} \frac{y_{on}}{n^2}\phi_n(x)\langle\phi_n, \epsilon_m\rangle + \left(\frac{d}{a}\right)^2 \sum_{n=1}^{\infty} \frac{y'_n}{n^2}\psi_n(x)\langle\psi_n, \epsilon_m\rangle = \bar{Y}\cdot\epsilon_m \tag{13}$$

where we have defined

$$\phi_n = \frac{2}{\sqrt{a}}\cos\frac{n\pi}{a}x; \quad \psi_n = \sqrt{\frac{2}{d}}\cos\frac{n\pi}{d}x$$

$$\epsilon_m(x) = \frac{a}{\pi}\frac{dE_m(x')}{dx'}; \quad \langle\phi_n, \epsilon_m\rangle = \int_0^d \phi_n \epsilon_m\, dx$$

and $\bar{Y}$ is the integral operator defined by (13).

Hence, formally, from (13),

$$\epsilon_m(x) = \frac{1}{m}\bar{Y}^{-1}\cdot\phi_m(x). \tag{14}$$

By the standard definition of open circuit impedance matrix of a multiport network, we obtain directly from (13) the impedance matrix as seen by the accessible ports, namely:

$$z_{km} = \langle e_k, E_m \rangle = -\left\langle \frac{\pi}{a} \int dx\, e_k(x), \frac{a}{\pi} \frac{dE_m(x')}{dx'} \right\rangle$$

$$= \frac{1}{k} \langle \phi_k, \epsilon_m \rangle = \frac{1}{mk} \langle \phi_k, \bar{Y}^{-1} \phi_m(x) \rangle. \quad (15)$$

The same formula, with the slight modification shown in the definition (8) of $y'_n$, applies to both the even and odd cases. The variational properties of (15) have been discussed before [8].

*Discretization of the Integral Equation*

The actual computation of the impedance matrix (15) takes place upon the discretization of the functions of $x$ and the operator $\bar{Y}$ appearing in the integral equation.

Upon consideration of the edge conditions at $x = d$, the discretization is achieved by means of a basis orthonormal on the aperture with respect to a weight function that expresses the singular behavior of the field there, that is:

$$W\left(\frac{x}{d}\right) = \left(1 - \left(\frac{x}{d}\right)^2\right)^{-(1/3)} \quad (16)$$

These basis functions are proportional to the Gegenbauer polynomial $G_n^{1/6}(x/d)$ with orthonormalization [10, p. 826]

$$\int_0^1 dt\, W(t)\, G_n^{1/6}(t)\, G_m^{1/6}(t) = N_m^2\, \delta_{nm} \quad (17)$$

$$N_m = \frac{2^{-(1/6)}}{\Gamma(\frac{1}{6})} \left[ \frac{\pi \Gamma(\frac{1}{3} + m)}{(\frac{1}{6} + m) m!} \right]^{1/2}.$$

Hence the desired orthonormal functions are given by

$$f_m(x) = \frac{1}{\sqrt{d}} \frac{1}{N_m} G_n^{1/6}\left(\frac{x}{d}\right): \quad m = 2, 4 \cdots \quad (18)$$

with orthonormalization

$$\langle f_m, Wf_n \rangle = \int_0^d f_m W f_n\, dx = \delta_{nm}. \quad (19)$$

It is noted that the choice of even polynomials and the even-to-$x$ behavior of $W$ complies with the electric wall boundary conditions at $x = 0$. Moreover, $n > 0$ due to the fact that (18) represents the $x$-derivative of the actual field.

In terms of the above basis, the functions $\phi_n$, $\psi_n$ (13) become respectively the vector $\underline{A}_n$ of components [10, p. 831]

$$A_{mn} = \langle f_m, W\phi_n \rangle$$

$$= 2\sqrt{\frac{d}{a}} \frac{1}{N_m} \int_0^1 dt \frac{G_m^{1/6}(t)}{\sqrt[3]{1 - t^2}} \cos \frac{n\pi d}{a} t$$

$$= 2\sqrt{r}\, c_m \frac{J_{m+1/6}(n\pi r)}{(n\pi r)^{1/6}}$$

$$m = 2, 4 \cdots, \; n = 1, 2, 3, 4 \cdots \quad (20)$$

with $r = d/a$,

$$c_m = (-1)^{m/2} \left[ \frac{\pi}{m!} \Gamma\left(\frac{1}{3} + m\right) \left(\frac{1}{6} + m\right) \right]^{1/2}$$

and $\underline{A}'_n$ of components

$$A'_{mn} = \langle f_m, W\psi_n \rangle$$

$$= \sqrt{2} \frac{1}{N_m} \int_0^1 dt \frac{G_m^{1/6}(t)}{\sqrt[3]{1 - t^2}} \cos n\pi t$$

$$= \sqrt{2}\, c_m \frac{J_{m+1/6}(n\pi)}{(n\pi)^{1/6}}$$

$$m = 2, 4 \cdots, \; n = 1, 3, 5 \cdots \quad (21)$$

while the operator $\bar{Y}$ becomes the matrix $\boldsymbol{Y}$ of components:

$$Y_{km} = \sum_{\substack{n > n_a \\ \text{odd}}}^{\infty} \frac{y_{on}}{n^2} A_{kn} A_{mn} + \sum_{n=1}^{\infty} \frac{y'_n}{n^2} A'_{kn} A'_{mn}. \quad (22)$$

The variational expression (15) of the reactance becomes

$$Z_{ij} = \frac{1}{ij} \underline{A}^T_{*i} \boldsymbol{Y}^{-1} \underline{A}_{*j} \qquad i, j = 1, 3, \cdots n_a. \quad (23)$$

The even/odd case impedances are calculated at each spot frequency by using the appropriate expression of $y'_n$ from (18). The $n_a$ + 1-port black box equivalent network of the symmetric post in the guide, shown in Fig. 2, is then recovered as

$$\frac{1}{2} \begin{bmatrix} \mathbf{Z}_e + \mathbf{Z}_o & \mathbf{Z}_e - \mathbf{Z}_o \\ \mathbf{Z}_e - \mathbf{Z}_o & \mathbf{Z}_e + \mathbf{Z}_o \end{bmatrix} \quad (24)$$

where $e$, $o$ denote the even/odd cases, respectively.

*Frequency Dependence of the Post*

Much more effective than computing (23) at each spot frequency, is, however, the technique of frequency extraction introduced in [9], leading, in fact, to a wideband, lumped, equivalent circuit for the post with frequency-independent elements.

It is noted that frequency enters the expression (23) of the impedance only via the modal characteristic admittances (6) and (7) of modes normally well below cutoff.

In the larger guide (width $a$), in fact, $n > n_a$. In case $TE_{10}$ in the smaller guide (width $d$) is also above cutoff, the argument below still applies by considering the discontinuity at $z = 0$ as a two-port step problem. The latter only involves a minor modification in the ensuing equivalent network.

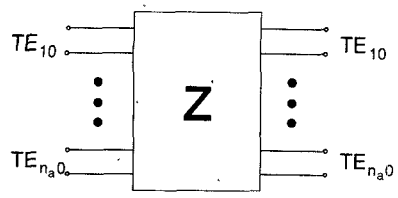


Fig. 2. "Black box" equivalent network for the accessible modes ($n = 1, 3, \cdots, n_a$).

It is also noted that, over the waveguide band, corresponding to $0 < \bar{\omega}_1 \le \bar{\omega} \le \bar{\omega}_2 < \sqrt{3}$[1] the following lumped approximation of $y_{on}$ is recovered by a modified first order expansion

$$y_{on} = \frac{\sqrt{n^2 - 1 - \bar{\omega}^2}}{j\bar{\omega}} = k_1^{(n)} \frac{\sqrt{n^2 - 1}}{j\bar{\omega}} + \frac{k_2^{(n)}}{2} \frac{j\bar{\omega}}{\sqrt{n^2 - 1}}. \tag{25}$$

The positive constants $k_1^{(n)}$, $k_2^{(n)}$ approach unity rapidly with increasing $n$ and can be set equal to unity for, say, $n \ge 5$.

These are determined by minimizing, in the minimum ripple sense, the maximum relative error function

$$\epsilon^n = \max_{\bar{\omega}_1 \le \bar{\omega} \le \bar{\omega}_2} \left| 1 - \frac{k_1^{(n)} \frac{\sqrt{n^2 - 1}}{j\bar{\omega}} + \frac{k_2^{(n)}}{2} \frac{j\bar{\omega}}{\sqrt{n^2 - 1}}}{\frac{\sqrt{n^2 - 1 - \bar{\omega}^2}}{j\bar{\omega}}} \right| \tag{26}$$

For instance, in the worst case ($n = 3$), we have $k_1^{(3)} = 1.006 k_2^{(3)} = 1.136$ corresponding to $\epsilon^3 = 2.258\ 10^{-3}$.

A stronger argument applies in narrower guide for the odd case, where we recover the lumped approximation:

$$y'_{on} \coth \gamma'_n s \approx k_{1s}^{(n)} \frac{\sqrt{n'^2 - 1}}{j\omega} \coth\left(\frac{\pi}{2}\frac{s}{a}\sqrt{n'^2 - 1}\right) + \frac{k_{2s}^{(n)}}{2} \frac{j\omega}{\sqrt{n'^2 - 1}} \left[ \frac{\coth\left(\frac{\pi}{2}\frac{s}{a}\sqrt{n'^2 - 1}\right)}{\sqrt{n'^2 - 1}} - \frac{\frac{\pi}{2}\frac{s}{a}}{\sinh^2\left(\frac{\pi}{2}\frac{s}{a}\sqrt{n'^2 - 1}\right)} \right] \tag{27a}$$

with $k_{is}^{(n)} = k_{is}^{(n)}(s, t, a)$.

[1]For example in the $K_A$ band $\bar{\omega}_1 = 0.7954$ $\bar{\omega}_2 = 1.6462$ (WR28 guide).

Regarding the approximation of $y'_1$ in the driving admittance under magnetic wall conditions at $z = s/2$, it is noted that the previous approach breaks down when the normalized length of the stub $s/a$ exceeds 0.4 and the normalized thickness $t/a \ll 1$. In this parameter range, the above model is valid over a narrower band. Long posts, however, occur only in the design of narrow band filters, so that the above model remains useful even in this case. It is noted that the best choice of the band edges $\bar{\omega}_1$, $\bar{\omega}_2$ of (26) for the approximation does coincide with the band of the filter.

Then the expression of $y'_1$ for the even case becomes

$$y'_{on} \tanh(\gamma'_n s) \approx k_{1o}^{(n)} \frac{\sqrt{n'^2 - 1}}{j\omega} \tanh\left(\frac{\pi}{2}\frac{s}{a}\sqrt{n^{+2} - 1}\right) + \frac{k_{2o}^{(n)}}{2} \frac{j\omega}{\sqrt{n'^2 - 1}} \frac{\tanh\left(\frac{\pi}{2}\frac{s}{a}\sqrt{n'^2 - 1}\right)}{\sqrt{n'^2 - 1}} + \frac{\frac{\pi}{2}\frac{s}{a}}{\cosh^2\left(\frac{\pi}{2}\frac{s}{a}\sqrt{n'^2 - 1}\right)} \tag{27b}$$

where $k_{io}^{(n)} = k_{io}^{(n)}(s, t, a)$ and is calculated minimizing the error function in the normalized band $1.45 \le \bar{\omega} \le 1.65$.

The advantage of the form above is in that they allow a frequency independent wide band equivalent circuit for the post to be extracted.

By substituting (25), (27) in (22) we may separate out the capacitive and inductive behaviors of $Y$ as follows.

Set

$$\boldsymbol{Y}(\bar{\omega}) = -j\boldsymbol{B}(\bar{\omega}) \tag{28}$$

with

$$\bar{\omega}\boldsymbol{B}(\bar{\omega}) = \boldsymbol{C}^s - \bar{\omega}^2\boldsymbol{C}^d \tag{29}$$

then the elements of $\boldsymbol{C}^s$, $\boldsymbol{C}^d$, constituting the inductive and capacitive contributions respectively, are given by

$$C^s_{km} = \sum_{\substack{n > n_a \\ \text{odd}}}^{\infty} k_1^{(n)} \frac{\sqrt{n^2 - 1}}{n^2} A_{kn} A_{mn} + r^2 \sum_{n=1}^{\infty} k_{1o/s}^{\prime(n)} \frac{\sqrt{n'^2 - 1}}{n^2} A'_{kn} A'_{mn} \cdot \begin{cases} \tanh\left(\frac{\pi}{2}\frac{s}{a}\sqrt{n'^2 - 1}\right) \\ \coth\left(\frac{\pi}{2}\frac{s}{a}\sqrt{n'^2 - 1}\right) \end{cases} \tag{30}$$

$$C^d_{km} = \frac{1}{2}\sum_{\substack{n>n_a\\ \text{odd}}}^{\infty} k_2^{(n)}\frac{\sqrt{n^2-1}}{n^2}A_{kn}A_{mn} + \frac{r^2}{2}\sum_{n=1}^{\infty} k'^{(n)}_{2o/s}\frac{\sqrt{n'^2-1}}{n^2}A'_{kn}A'_{mn} \cdot \left\{ \frac{\tanh\left(\frac{\pi}{2}\frac{s}{a}\sqrt{n'^2-1}\right)}{\sqrt{n'^2-1}} + \frac{\frac{\pi}{2}\frac{s}{a}}{\coth^2\left(\frac{\pi}{2}\frac{s}{a}\sqrt{n'^2-1}\right)} \right. \left. \frac{\coth\left(\frac{\pi}{2}\frac{s}{a}\sqrt{n'^2-1}\right)}{\sqrt{n'^2-1}} - \frac{\frac{\pi}{2}\frac{s}{a}}{\sinh^2\left(\frac{\pi}{2}\frac{s}{a}\sqrt{n'^2-1}\right)} \right\}. \quad (31)$$

Since $\boldsymbol{C}^s$, $\boldsymbol{C}^d$ are real, symmetric matrices and $\boldsymbol{C}^s$, at least, is positive definite, we can diagonalize them simultaneously and invert the susceptance matrix $\boldsymbol{B}$. Recalling the concept of "square root" of a non-negative matrix, we extract the factor $(\boldsymbol{C}^s)^{1/2}$ to the left and to the right of (29), that is,

$$\begin{aligned}\bar{\omega}\boldsymbol{B}(\bar{\omega}) &= (\boldsymbol{C}^s)^{1/2}[\boldsymbol{I} - \bar{\omega}^2(\boldsymbol{C}^s)^{-1/2}\,\boldsymbol{C}^d(\boldsymbol{C}^s)^{-1/2}](\boldsymbol{C}^s)^{1/2}\\ &= (\boldsymbol{C}^s)^{1/2}[\boldsymbol{I} - \bar{\omega}^2\boldsymbol{T}\boldsymbol{\Lambda}\boldsymbol{T}^t](\boldsymbol{C}^s)^{1/2}\\ &= \boldsymbol{M}^{-1}[\boldsymbol{I} - \bar{\omega}^2\boldsymbol{\Lambda}](\boldsymbol{M}^{-1})^t) \quad (32)\end{aligned}$$

where we have set

$$(\boldsymbol{C}^s)^{-1/2}\boldsymbol{C}^d(\boldsymbol{C}^s)^{-1/2} = \boldsymbol{T}\boldsymbol{\Lambda}\boldsymbol{T}^t \quad (33)$$

$\boldsymbol{T}$ being the orthogonal matrix of the eigenvectors of (33), $\boldsymbol{\Lambda} = \text{diag}\,(1/\bar{\omega}_m^2)$ the diagonal matrix of its positive eigenvalues and $\boldsymbol{I}$ the unit matrix. The apex $t$ denotes transposition. Moreover, we have defined

$$\boldsymbol{M}^{-1} = (\boldsymbol{C}^s)^{1/2}\boldsymbol{T}. \quad (34)$$

Having cast $\boldsymbol{B}$ in the form (32) we are now in a position to recover its inverse analytically, while keeping its frequency dependence explicit, that is, from (32)

$$\boldsymbol{B}^{-1}(\bar{\omega}) = \bar{\omega}(\boldsymbol{M})^t[\boldsymbol{I} - \bar{\omega}^2\boldsymbol{\Lambda}]^{-1}\boldsymbol{M} \quad (35)$$

Finally, substituting now (35) in the variational expression (23), we recover the post reactance $X(\bar{\omega}) = -jZ(\bar{\omega})$ with explicit frequency dependence, namely, elementwise,

$$\begin{aligned}X_{kj}(\bar{\omega}) &= \frac{\bar{\omega}}{kj}\underline{A}'_{*k}(\boldsymbol{M})^t[\boldsymbol{I} - \bar{\omega}^2\boldsymbol{\Lambda}]^{-1}\boldsymbol{M}\underline{A}_{*j}\\ &= \frac{\bar{\omega}}{kj}\sum_{m=0}^{N-1}\frac{(\boldsymbol{M}\underline{A}_{*k})_m(\boldsymbol{M}\underline{A}_{*j})_m}{1-\left(\frac{\bar{\omega}}{\bar{\omega}_m}\right)^2}\\ &= \bar{\omega}\sum_{m=0}^{N-1}\frac{r_{kj}^{(m)}}{1-\left(\frac{\bar{\omega}}{\bar{\omega}_m}\right)^2} \qquad 1 \le k, j \le n_a. \quad (36)\end{aligned}$$

This is the canonical Foster's form of the even/odd case post reactance expressed in terms of $N$ poles, $\bar{\omega}_m$, rapidly increasing with $m$: $M = 0, 1 \cdots N-1$ and their corresponding residues $r^{(m)}$.

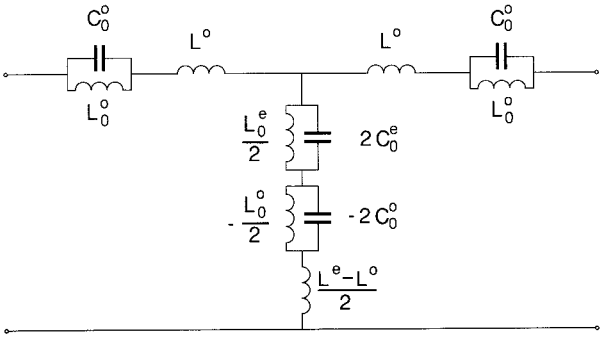


Fig. 3 Lumped equivalent circuit of the post.

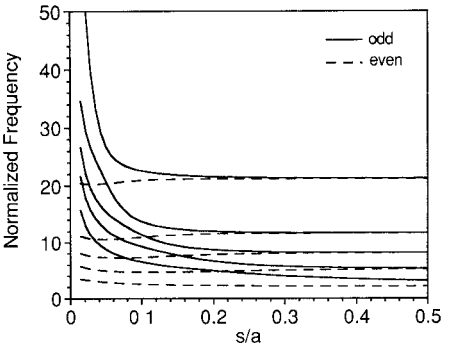


Fig. 4. Normalized poles versus $s/a$ for $t/a = 0.021$ and $N = 5$.

TABLE I
NORMALIZED FIRST TWO POLES AND COMPUTER TIMES FOR TWO TYPICAL POSTS/($t/a = 0.021$; $s/a = 0.0281$ (1) AND $s/a = 0.492$ (2))

| | 1 | | 2 | | |
|---|---|---|---|---|---|
| $N$ | even | odd | even | odd | $t$ (sec) |
| 1 | 3.6057 | 24.619 | 2.2261 | 3.3972 | 1.7 |
| 2 | 3.2248 | 11.383 | 2.1138 | 3.1729 | 3.9 |
| 3 | 3.2019 | 11.351 | 2.1117 | 3.1669 | 9.2 |
| 4 | 3.2017 | 11.329 | 2.1117 | 3.1669 | 19.3 |
| 5 | 3.2017 | 11.326 | 2.1117 | 3.1669 | 32.4 |

Apart from the first and, possibly, the second pole, the rest can be neglected and the reactance expressed in terms of a dynamic term and, possibly, a quasi-static inductive remainder.

The equivalent circuit of (36) is shown in Fig. 3 where just the first resonant term is actually drawn ($m = 0$). Distributed circuits, more complex than the one above, but yielding greater precision for thin, long posts over over the whole band, are also possible.

## RESULTS

Fig. 4 shows the location of the first 5 poles of expression (36) versus the normalized post length. This is a convergence check showing that, in order to obtain satisfactory results, it is sufficient to take the first two or, at the most three, poles. It is noted that, as $s/a$ increases, poles of the even and odd mode circuits become alike, as the section below cutoff is so long that reflection does not depend on termination. In Table I the reader can find values of the dominant poles, calculated by using $N$ expan-

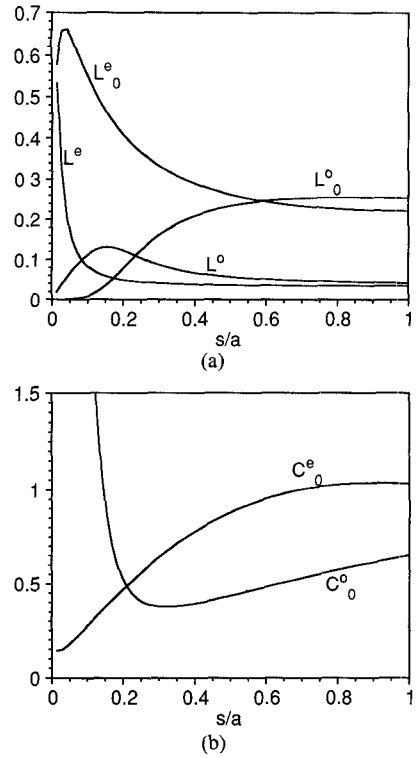


Fig. 5. (a) Lumped inductances for $t/a = 0.021$ and $N = 2$. (b) Lumped capacitances for $t/a = 0.021$ and $N = 2$.

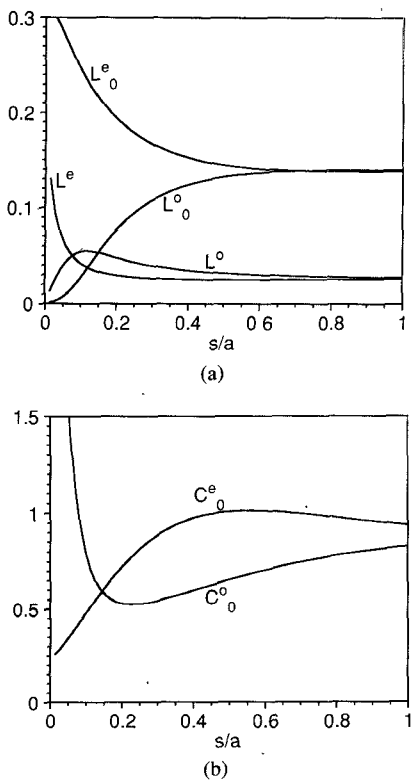


Fig. 6. (a) Lumped inductances for $t/a = 0.141$ and $N = 2$. (b) Lumped capacitances for $t/a = 0.141$ and $N = 2$.

sion functions, and computer times required for their evaluation on a hp 9000 835 machine with NAG mathematical library.

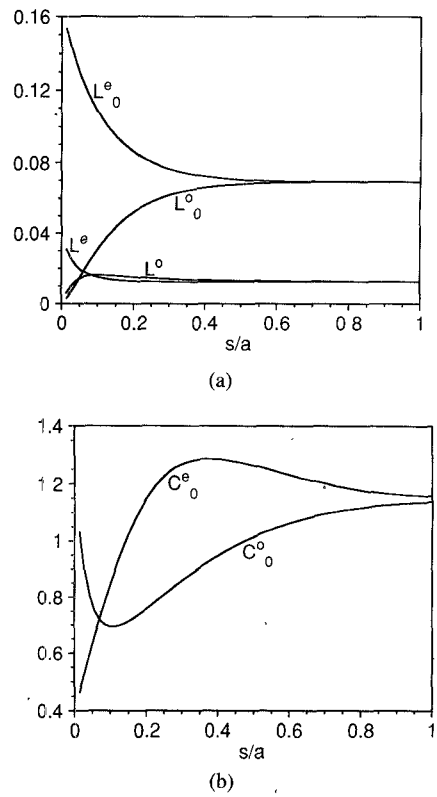


Fig. 7. (a) Lumped inductances for $t/a = 0.281$ and $N = 2$. (b) Lumped capacitances for $t/a = 0.281$ and $N = 2$.

Element values $L$ and $C$, for different normalized thicknesses and normalized lengths of the post are reported in Figs. 5–7. Comparing these figures, it can be seen that as the thickness increases, $L$ decreases as the post becomes similar to a short circuit.

For the ease of reference, the same parameters as in Figs. 5–7 are listed in Tables II–IV. Using the above set of values and interpolating between them, the reader can set up his own accurate analysis program for cascades of inductive posts without any recourse to field modeling.

Figs. 8 and 9 show magnitudes of transmission coefficients for a cascade of two post separated by distances $u$, $2u$, $3u$, 4u ($u = l/a = 0.14$). In the first figure $s/a = 0.492$, in the second $s/a = 0.028$. Continuous curves were calculated taking into account the mutual interaction between two posts through the first higher order mode of the guide that is below cutoff. The results obtained neglecting this effect are shown by the broken curves. We note that there is an appreciable difference only when the post length is short enough ($l/a < 0.3$).

The larger selectivity of longer posts with respect to shorter ones is evident. The theory discussed above was applied to the analysis of $E$-plane filters. Fig. 10 shows a section of the structure, $l$ denotes the length of a section of empty guide $s$ is the length of a post.

Figs. 11–13 compare experimental and theoretical results for reflection end transmission of the three filters whose dimensions are listed in Table V. Continuous curves are calculated taking into account the interactions

TABLE II
LUMPED INDUCTANCES AND CAPACITANCES FOR $t/a = 0.021$ AND $N = 2$
(FOR A WR28 WAVEGUIDE ($a = 7.112$ mm) $s$ INCREASES BY STEPS OF 0.1)

| $s/a$ | $L_0^e$ | $L_0^o$ | $C_0^e$ | $C_0^o$ | $L^e$ | $L^o$ |
|---|---|---|---|---|---|---|
| 0.01406 | 0.5791 | 0.0001073 | 0.1410 | 37.49 | 0.5337 | 0.01957 |
| 0.02812 | 0.6577 | 0.0003540 | 0.1464 | 21.80 | 0.3086 | 0.03820 |
| 0.04218 | 0.6614 | 0.0008438 | 0.1663 | 13.16 | 0.2034 | 0.05571 |
| 0.05624 | 0.6401 | 0.001718 | 0.1909 | 8.270 | 0.1487 | 0.07191 |
| 0.09843 | 0.5536 | 0.008684 | 0.2731 | 2.568 | 0.08362 | 0.1107 |
| 0.1406 | 0.4820 | 0.02744 | 0.3567 | 1.076 | 0.06178 | 0.1300 |
| 0.1828 | 0.4278 | 0.06081 | 0.4382 | 0.6073 | 0.05174 | 0.1280 |
| 0.2250 | 0.3863 | 0.1009 | 0.5159 | 0.4466 | 0.04624 | 0.1134 |
| 0.2672 | 0.3540 | 0.1376 | 0.5887 | 0.3916 | 0.04288 | 0.09737 |
| 0.3093 | 0.3286 | 0.1670 | 0.6558 | 0.3772 | 0.04068 | 0.08441 |
| 0.3515 | 0.3081 | 0.1896 | 0.7167 | 0.3806 | 0.03916 | 0.07485 |
| 0.3937 | 0.2916 | 0.2069 | 0.7712 | 0.3923 | 0.03806 | 0.06777 |
| 0.4359 | 0.2781 | 0.2200 | 0.8195 | 0.4084 | 0.03725 | 0.06249 |
| 0.4781 | 0.2671 | 0.2300 | 0.8618 | 0.4268 | 0.03663 | 0.05845 |
| 0.5202 | 0.2580 | 0.2375 | 0.8985 | 0.4462 | 0.03616 | 0.05528 |
| 0.5624 | 0.2505 | 0.2432 | 0.9300 | 0.4662 | 0.03578 | 0.05275 |
| 0.6046 | 0.2442 | 0.2473 | 0.9569 | 0.4863 | 0.03549 | 0.05070 |
| 0.6468 | 0.2391 | 0.2503 | 0.9793 | 0.5063 | 0.03527 | 0.04899 |
| 0.6890 | 0.2350 | 0.2524 | 0.9977 | 0.5259 | 0.03509 | 0.04756 |
| 0.7312 | 0.2316 | 0.2537 | 1.012 | 0.5451 | 0.03495 | 0.04636 |
| 0.7733 | 0.2288 | 0.2545 | 1.023 | 0.5637 | 0.03486 | 0.04531 |
| 0.8155 | 0.2267 | 0.2549 | 1.031 | 0.5818 | 0.03479 | 0.04442 |
| 0.8577 | 0.2250 | 0.2549 | 1.035 | 0.5992 | 0.03476 | 0.04364 |
| 0.8999 | 0.2237 | 0.2546 | 1.037 | 0.6159 | 0.03474 | 0.04294 |
| 0.9421 | 0.2228 | 0.2541 | 1.036 | 0.6319 | 0.03475 | 0.04234 |
| 0.9843 | 0.2221 | 0.2535 | 1.034 | 0.6473 | 0.03478 | 0.04180 |

TABLE III
LUMPED INDUCTANCES AND CAPACITANCES FOR $t/a = 0.141$ AND $N = 2$
(FOR A WR28 WAVEGUIDE ($a = 7.112$ mm) $s$ INCREASES BY STEPS OF 0.1)

| $s/a$ | $L_0^e$ | $L_0^o$ | $C_0^e$ | $C_0^o$ | $L^e$ | $L^o$ |
|---|---|---|---|---|---|---|
| 0.01406 | 0.3050 | 0.001083 | 0.2586 | 3.248 | 0.1301 | 0.01341 |
| 0.02812 | 0.3012 | 0.002830 | 0.2904 | 2.398 | 0.09428 | 0.02505 |
| 0.04218 | 0.2916 | 0.005446 | 0.3260 | 1.809 | 0.07374 | 0.03476 |
| 0.05624 | 0.2802 | 0.009085 | 0.3632 | 1.404 | 0.06088 | 0.04242 |
| 0.09843 | 0.2469 | 0.002610 | 0.4767 | 0.8049 | 0.04192 | 0.05394 |
| 0.1406 | 0.2205 | 0.04817 | 0.5854 | 0.6047 | 0.03414 | 0.05374 |
| 0.1828 | 0.2004 | 0.06910 | 0.6845 | 0.5398 | 0.03029 | 0.04955 |
| 0.2250 | 0.1853 | 0.08630 | 0.7705 | 0.5255 | 0.02815 | 0.04511 |
| 0.2672 | 0.1737 | 0.09967 | 0.8418 | 0.5328 | 0.02689 | 0.04144 |
| 0.3093 | 0.1649 | 0.1099 | 0.8982 | 0.5499 | 0.02611 | 0.03857 |
| 0.3515 | 0.1581 | 0.1176 | 0.9407 | 0.5715 | 0.02562 | 0.03635 |
| 0.3937 | 0.1529 | 0.1234 | 0.9711 | 0.5949 | 0.02531 | 0.03461 |
| 0.4359 | 0.1489 | 0.1278 | 0.9918 | 0.6189 | 0.02514 | 0.03324 |
| 0.4781 | 0.1459 | 0.1311 | 1.004 | 0.6426 | 0.02505 | 0.03216 |
| 0.5202 | 0.1436 | 0.1335 | 1.011 | 0.6653 | 0.02500 | 0.03127 |
| 0.5624 | 0.1419 | 0.1354 | 1.013 | 0.6868 | 0.02500 | 0.03053 |
| 0.6046 | 0.1406 | 0.1367 | 1.011 | 0.7070 | 0.02504 | 0.02993 |
| 0.6468 | 0.1396 | 0.1377 | 1.006 | 0.7259 | 0.02509 | 0.02943 |
| 0.6890 | 0.1390 | 0.1383 | 1.000 | 0.7433 | 0.02516 | 0.02900 |
| 0.7312 | 0.1385 | 0.1388 | 0.9927 | 0.7591 | 0.02524 | 0.02865 |
| 0.7733 | 0.1382 | 0.1391 | 0.9842 | 0.7736 | 0.02533 | 0.02834 |
| 0.8155 | 0.1380 | 0.1393 | 0.9754 | 0.7867 | 0.02542 | 0.02808 |
| 0.8577 | 0.1379 | 0.1395 | 0.9665 | 0.7985 | 0.02552 | 0.02786 |
| 0.8999 | 0.1378 | 0.1395 | 0.9578 | 0.8090 | 0.02562 | 0.02767 |
| 0.9421 | 0.1378 | 0.1396 | 0.9495 | 0.8183 | 0.02571 | 0.02750 |
| 0.9843 | 0.1378 | 0.1395 | 0.9422 | 0.8267 | 0.02580 | 0.02737 |

between posts and three function (pole) expansions, broken curves utilize a simplified model (single pole, no interaction). As can be seen, the agreement between theoretical and experimental results is very good, indeed, considering mechanical tolerances of the prototype and measurement errors.

Utilizing the simple equivalent network of Fig. 3 with element values given in Figs. 5–7 yields results that are

TABLE IV
LUMPED INDUCTANCES AND CAPACITANCES FOR $t/a = 0.281$ AND $N = 2$
(FOR A WR28 WAVEGUIDE ($a = 7.112$ mm) $s$ INCREASES BY STEPS OF 0.1)

| $s/a$ | $L_0^e$ | $L_0^o$ | $C_0^e$ | $C_0^o$ | $L^e$ | $L^o$ |
|---|---|---|---|---|---|---|
| 0.01406 | 0.1536 | 0.003126 | 0.4628 | 1.032 | 0.03087 | 0.006107 |
| 0.02812 | 0.1432 | 0.007091 | 0.5300 | 0.8946 | 0.02486 | 0.01036 |
| 0.04218 | 0.1344 | 0.01164 | 0.5961 | 0.8060 | 0.02121 | 0.01309 |
| 0.05624 | 0.1267 | 0.01646 | 0.6606 | 0.7513 | 0.01882 | 0.01472 |
| 0.09843 | 0.1091 | 0.03027 | 0.8408 | 0.6947 | 0.01514 | 0.01617 |
| 0.1406 | 0.09708 | 0.04126 | 0.9926 | 0.7065 | 0.01365 | 0.01586 |
| 0.1828 | 0.08881 | 0.04937 | 1.110 | 0.7410 | 0.01296 | 0.01527 |
| 0.2250 | 0.08302 | 0.05522 | 1.192 | 0.7830 | 0.01261 | 0.01474 |
| 0.2672 | 0.07893 | 0.05939 | 1.245 | 0.8263 | 0.01245 | 0.01431 |
| 0.3093 | 0.07605 | 0.06236 | 1.273 | 0.8681 | 0.01237 | 0.01397 |
| 0.3515 | 0.07399 | 0.06447 | 1.286 | 0.9071 | 0.01235 | 0.01371 |
| 0.3937 | 0.07254 | 0.06596 | 1.286 | 0.9425 | 0.01235 | 0.01350 |
| 0.4359 | 0.07151 | 0.06701 | 1.280 | 0.9741 | 0.01237 | 0.01334 |
| 0.4781 | 0.07079 | 0.06775 | 1.270 | 1.002 | 0.01239 | 0.01321 |
| 0.5202 | 0.07030 | 0.06827 | 1.258 | 1.026 | 0.01242 | 0.01311 |
| 0.5624 | 0.06997 | 0.06862 | 1.244 | 1.047 | 0.01246 | 0.01303 |
| 0.6046 | 0.06976 | 0.06886 | 1.230 | 1.065 | 0.01249 | 0.01296 |
| 0.6468 | 0.06963 | 0.06903 | 1.217 | 1.080 | 0.01252 | 0.01291 |
| 0.6890 | 0.06955 | 0.06913 | 1.205 | 1.093 | 0.01255 | 0.01287 |
| 0.7312 | 0.06951 | 0.06920 | 1.193 | 1.103 | 0.01258 | 0.01283 |
| 0.7733 | 0.06950 | 0.06925 | 1.184 | 1.112 | 0.01260 | 0.01281 |
| 0.8155 | 0.06950 | 0.06928 | 1.175 | 1.120 | 0.01263 | 0.01278 |
| 0.8577 | 0.06949 | 0.06930 | 1.169 | 1.126 | 0.01264 | 0.01277 |
| 0.8999 | 0.06950 | 0.06931 | 1.164 | 1.130 | 0.01266 | 0.01275 |
| 0.9421 | 0.06949 | 0.06932 | 1.161 | 1.134 | 0.01267 | 0.01274 |
| 0.9843 | 0.06949 | 0.06932 | 1.158 | 1.137 | 0.01267 | 0.01273 |

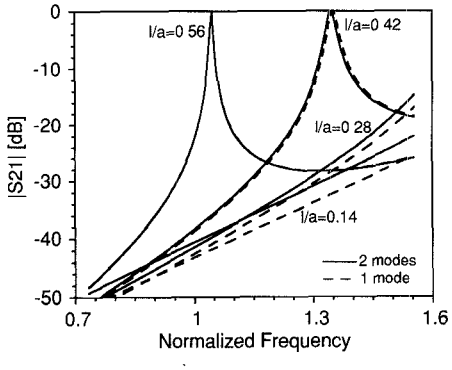


Fig. 8. Magnitude of transmission coefficient of two posts for $t/a = 0.021$ and $s/a = 0.492$.

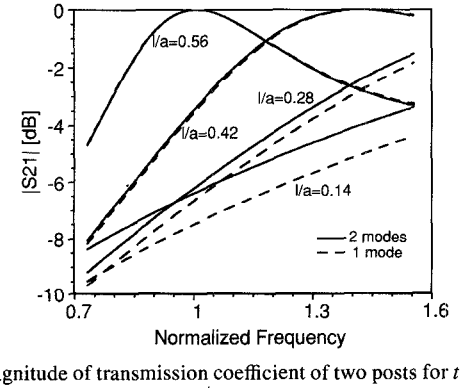


Fig. 9. Magnitude of transmission coefficient of two posts for $t/a = 0.021$ and $s/a = 0.028$.

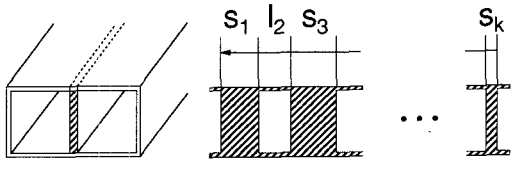


Fig. 10. Millimeter-wave $E$-plane metal insert filters.

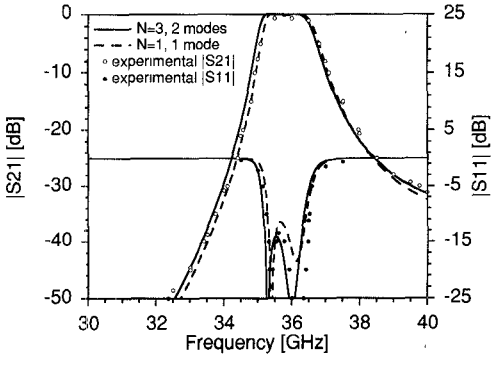


Fig. 11. Theoretical and experimental response of filter 1.

virtually indistinguishable at midband from those of the more accurate model but differing slightly towards the upper band edge due to the effect of higher order mode interaction.

Finally, the computer time involved in the analysis of the more complicated filter 2, that comprises the characterization of all posts with a $3 \times 3$ model and their mutual

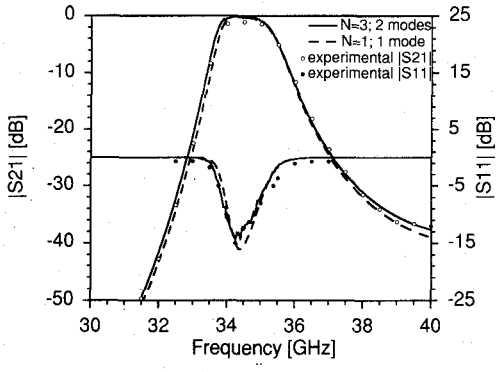


Fig. 12. Theoretical and experimental response of filter 2.

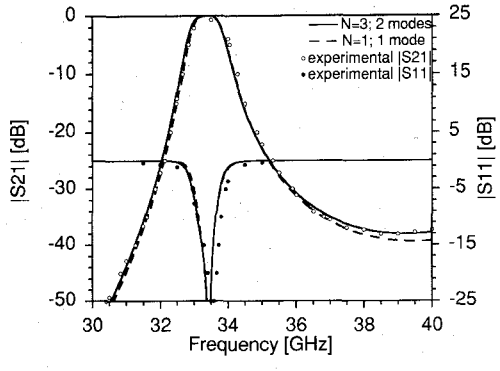


Fig. 13. Theoretical and experimental response of filter 3.

TABLE V
DATA (IN mm) OF THREE TYPICAL FILTERS (THE WAVEGUIDE IS A WR28 WORKING IN THE $K_A$ BAND)

| Length | Filter 1 | Filter 2 | Filter 3 |
|---|---|---|---|
| $s_1$ | 1.015 | 0.283 | 0.667 |
| $l_2$ | 3.442 | 3.757 | 4.143 |
| $s_3$ | 3.587 | 2.328 | 3.341 |
| $l_4$ | 3.449 | 3.809 | 4.148 |
| $s_5$ | 3.587 | 3.526 | 3.341 |
| $l_6$ | 3.442 | 3.809 | 4.143 |
| $s_7$ | 1.015 | 2.328 | 0.667 |
| $l_8$ | — | 3.757 | — |
| $s_9$ | — | 0.283 | — |
| $t$ | 0.15 | 0.15 | 0.15 |

interaction for 201 points of frequency, was about 34 s of CPU on a hp 9000 835 series machine.

## CONCLUSION

We have investigated the problem of inductive posts of arbitrary thickness in rectangular waveguide, inclusive of near neighbor interaction by a combination of fields and network methods.

By introducing the correct 90°-edge condition in the field solution, matrix sizes are kept to a maximum of three by three, thus achieving substantial computer time savings (typically by a factor of five).

Moreover, we were able to separate out and extract analytically frequency and geometry dependences, yielding true wideband equivalent circuits for the post with frequency independent elements. This result eliminates the need to repeat the field analysis at each frequency point and enhances still further the speed of the analysis.

Lumped element values are plotted vs. post width for various post thicknesses. By using the above curves and interpolating between them, the reader can set up his own accurate analysis program for cascade of posts without recourse to any field modeling at all. Finally, theoretical results are in excellent agreement with experimental data for three different multipost filters at $K_A$ band.

## REFERENCES

[1] Y. Konishi and K. Uenakada, "The design of a bandpass filter with inductive strip-planar circuit mounted in waveguide," *IEEE Trans. Microwave Theory Tech.*, vol. MTT-22, no. 10, pp. 869–873, Oct. 1974.

[2] F. Arndt, J. Bornemann, R. Vahldieck, and D. Grauerholz, "E plane integrated circuit filters with improved stopband attenuation," *IEEE Trans. Microwave Theory Tech.*, vol. MTT-32, no. 10, pp. 1391–1394, Oct. 1984.

[3] Y. Shih and T. Ihoh, "E-plane filters with finite-thickness septa," *IEEE Trans. Microwave Theory Tech.*, vol. MTT-31, no. 12, pp. 1009–1013, Dec. 1983.

[4] Y. Shih, "Design of waveguide E-plane filters with all-metal inserts," *IEEE Trans. Microwave Theory Tech.*, vol. MTT-32, no. 7, pp. 1009–1013, July 1984.

[5] L. Q. Bui, D. Ball, and T. Itoh, "Broad-band millimeter-wave E-plane bandpass filters," *IEEE Trans. Microwave Theory Tech.*, vol. MTT-32, no. 12, pp. 1655–1658, Dec. 1984.

[6] R. Vahldieck and W. J. R. Hoefer, "Finline and metal insert filters with improved passband separation and increased stopband attentuation," *IEEE Trans. Microwave Theory Tech.*, vol. MTT-33, no. 12, pp. 1333–1339, Dec. 1985.

[7] R. Mansour and R. H. Macphie, "An improved transmission matrix formulation of cascaded discontinuities and its application to E-plane circuits," *IEEE Trans. Microwave Theory Tech.*, vol. MTT-34, no. 12, pp. 1490–1498, Dec. 1986.

[8] T. Rozzi, "Network analysis of strongly coupled transverse apertures in waveguide," *Int. J. Circuit Theory Appl.*, vol. 1, pp. 161–179, 1972.

[9] T. Rozzi and W. Mecklenbräuker, "Wide-band network modeling of interacting inductive irises and steps," *IEEE Trans. Microwave Theory Tech.*, vol. MTT-23, no. 2, pp. 235–245, Feb. 1975.

[10] I. S. Gradshtein and I. M. Rhyzik, *Table of Integrals Series, and Products*. New York: Academic, 1965.

**Tullio Rozzi** (M'66–SM'74–F'90) was born in Italy in 1941. He obtained the degree of "dottore" in physics from Pisa University in 1965, the Ph.D. degree in electrical engineering from Leeds University in 1968, and the D.Sc. degree from the University of Bath in 1987.

From 1968 to 1978 he was a Research Scientist at the Philips Research Laboratories, Eindhoven, The Netherlands, having spent one year, 1975, at the Antenna Laboratory, University of Illinois, Urbana. In 1978 he was appointed to Chair of Electrical Engineering at University of Liverpool, U.K., and subsequently was appointed to the Chair of Electronics and Head of the Electronics Group at the University of Bath in 1981. From 1983 to 1986 he held the additional responsibility of Head of School of Electrical Engineering at Bath. Since 1986 he has held the Chair of Antennas at the Faculty of Engineering, University of Ancona, Italy, while remaining a Visiting Professor at Bath.

In 1975 Dr. Rozzi was awarded the Microwave Prize by the Microwave Theory and Techniques Society of the IEEE. He is a Fellow of the IEE (U.K.).

**Franco Moglie** (M'91) was born in Ancona, Italy, in 1961. He received the degree of "dottore ingegnere" in Electronics Engineering from the University of Ancona, Italy, in 1986.

Since 1986 he has been a Tenured Researcher with the "Dipartimento di Elettronica ed Automatica" at the University of Ancona. His work is mainly in the area of microwave and millimeter techniques and hyperthermia applicators.

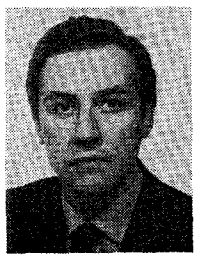

**Antonio Morini** was born in Italy in 1962. He received the degree of "dottore ingegnere" in electronics engineering from the University of Ancona in 1987.

Since 1988 he has been with the "Dipartimento di Elettronica ed Automatica" at the University of Ancona as a Research Assistant. His research is mainly devoted to the modeling of passive millimetric wave devices and antennas.

**William James Gulloch** was born in Wick, Scotland in 1958. He received the degree of B.Sc. in computational physics from Heriot-Watt University, Edinburgh, Scotland in 1982.

After working for Texas Instruments Ltd., England for one year he joined M/A-COM Ltd., England as a Microwave Engineer. In 1986 he was transferred to the Advanced Technology Department where he worked on various millimeter wave components, including multipliers, switches and limiters. In 1989 he moved to Elettronica S.p.a., Italy, where he worked as Principle Engineer on EW components. Since 1990 he has been working for Telettra S.p.a., Italy as Group Leader of the Millimeter Wave Group, where he is currently developing a 38 GHz communications system.

**Marco Politi** was born in Milan, Italy, in 1962. He received the degree (summa cum laude) in electronics engineering from the University of Trieste, Italy, in 1988. His thesis, on the nonlinear behavior and computer simulation of GaAs MESFET devices, was developed at Telettra S.p.A., Vimercate, Italy.

He joined Telettra S.p.a. in the same year as a Design Engineer of linear and nonlinear microwave subsystems. After having served with the Italian Army as an Officer of the Corpo Tecnico in Rome, he is currently with Telettra, Digital Radio Links Department—Millimeter Wave Group, dealing with the development of a 38 GHz system for PCN applications.